International Journal on Advanced Science Engineering Information Technology

Vol.7 (2017) No. 1
ISSN: 2088-5334

Target Localization in MIMO OFDM Radars Adopting Adaptive Power Allocation among Selected Sub-Carriers

I. Pasya[#], T. Kobayashi[*], M. F. Abdul Khalid[#], N. Ab Wahab[#], N. E. A. Rashid[#], Z. Awang[#]

[#]*Microwave Research Institute, Universiti Teknologi MARA, 40450 Shah Alam, Selangor, Malaysia*
E-mail: idnin@salam.uitm.edu.my, mfarid044@salam.uitm.edu.my, norfishah@ieee.org, emileen98@salam.uitm.edu.my, zaiki437@salam.uitm.edu.my

[*]*Wireless Systems Laboratory, Tokyo Denki University, 5 Senju-Asahi-Cho, Tokyo 120-8851, Japan*
E-mail: koba@c.dendai.ac.jp

Abstract*— Multiple-input multiple-output (MIMO) radar has been introduced to enhance the performance of classical radar systems. Nevertheless, radar cross sections (RCS) fluctuations remains a known problem in radars. Target localization using narrowband signal produces reduced accuracy due to RCS fluctuations. One of the solutions to this problem is the utilization of frequency diversity of wideband signal. This paper presents target localization in MIMO radars using an adaptive orthogonal frequency division multiplexing (OFDM) waveform for effective frequency diversity utilization. Each transmitting antenna transmits an OFDM signal in different time slots and received by the each receiving antenna in the receiver array. A joint direction-of-departure (DOD) and direction-of-arrival (DOA) estimation scheme is applied to each of the OFDM sub-carrier using two-way multiple signal classification (MUSIC) algorithm. The estimation results at each sub-carrier are combined based on majority decision using angle histogram (non-parametric approach) to formulate the final wideband angle estimation. In addition, an adaptive power allocation among the sub-carriers is implemented, where the system evaluates the signal quality at each sub-carrier and consequently formulates a feedback to the MIMO transmitting side. The following transmission will comprise of OFDM waveform that focuses the transmit power at selected sub-carriers only. The sub-carrier selection is based on singular values obtained from singular value decomposition operation at each of the sub-carrier. The performance of the proposed scheme is evaluated through numerical simulations as well as validation by experiments in a radio anechoic chamber. It was demonstrated that the usage of a larger number of sub-carriers improves the angle estimation accuracy.

***Keywords*— MIMO radars; OFDM; DOD; DOA; MUSIC; radar cross section; power allocation; sub-carrier selection**

I. INTRODUCTION

Radars deal with many different and diverse problems. However, most radar systems are generally designed for the purpose of detecting the presence or absence of targets and estimating their range, velocity, and location. The most basic form of a radar system consists of a single pair of transmitter and receiver that can be positioned either in monostatic or bistatic geometry. As the development of the technology progressed, more complicated forms of radars that comprising multiple antennas and radar sites emerged such as multi-static and phase array radars. The multi-static radars operate multiple pairs of independent monostatic radars which are distributed in space. The phase array radars use multiple transmitting antennas that emit similar waveforms simultaneously and are capable of cohering and steering the antenna beam into a desired direction.

In recent years, radars utilizing multiple antennas at both the transmitter and receiver side have been proposed which are referred to as multiple-input multiple-output (MIMO) radars [1]-[3]. A MIMO radar system transmits independent signals that are orthogonal, correlated or partially correlated with each other where careful selection would increase its degree of freedom compared to the conventional phased array radar that uses the same number of antennas [2], [4]. Early works on MIMO radar indicated that the increase degree of freedom induces various benefits for target localization such as improvement of a number of detectable targets, resolution, and robustness against radar cross section (RCS) fluctuation [5], [6].

Various target localization schemes for MIMO radar has been proposed [7]-[9]. Nevertheless, many of them only consider narrowband signal. Target localization using narrowband signal tends to suffer from RCS fluctuations of a target, which causes signal fading that may reduce the localization accuracy [10], [11]. In order to reduce the effects of RCS fluctuations on localization accuracy, several solutions have been proposed. For example, using adaptive

waveform design that incorporates the target's RCS characteristics into a feed-back loop system [12] and usage of wideband signal that averages the channel information among different frequencies. The method proposed in [10] presented the usage of orthogonal frequency division multiplexing (OFDM) scheme in estimating the DOA of the targets. However, only one-dimensional angle estimation using a limited number of sub-carriers was discussed. The authors have previously reported an angle estimation scheme utilizing frequency diversity of an ultra-wideband (UWB) signal in MIMO radar, where the UWB signal was treated as a summation of sinusoidal waves swept throughout the UWB bandwidth [13]. The scheme estimated the target angle at each of the frequency components and combined them to increase the estimation accuracy.

The present paper proposes a joint direction-of-departure (DOD) and direction-of-arrival (DOA) estimation scheme in ultra-wideband (UWB) MIMO radar using OFDM waveform. The wideband OFDM waveform allows the radar to take advantage of independent information carried by each of the OFDM sub-carriers, which can be exploited to increase the estimation accuracy. The proposed scheme opted a two-dimensional multiple signal classification (MUSIC) algorithm [14] to jointly estimate the DOD and DOA at each of the sub-carrier of the OFDM signal. These estimates were then combined to compute the final wideband DOD and DODA estimation by means of majority decision technique. A non-parametric approach using histograms of the estimated angles was used to carry out the majority decision [13]. This approach enabled us to use a large number of sub-carriers that without affecting the estimation performance. The proposed scheme was validated through numerical simulations as well as experimental evaluations in a radio anechoic chamber.

The remainder of this paper is organized as follows. Section II describes the proposed scheme, Section III presents parameters and results of numerical simulations, and Section IV explained the experimental setup and the measured results. The concluding remarks are presented in Section V of the paper.

II. Material and Method

MIMO radar comprises of *M* transmitting and *N* receiving antennas illuminating a far-field target is considered, as illustrated in Fig. 1. The transmitting and receiving antennas of the MIMO radar are positioned in a uniform linear array with inter-element spacing of a half wavelength. Since the antennas are co-located, each transmit-receive antenna pairs are considered to observe the same aspect angle of the target. The MIMO radar transmits OFDM waveforms as the probing signal, each of which consists of H number of sub-carriers. Each sub-carrier carries randomly generated baseband data which were modulated with binary phased shift keying (BPSK) scheme.

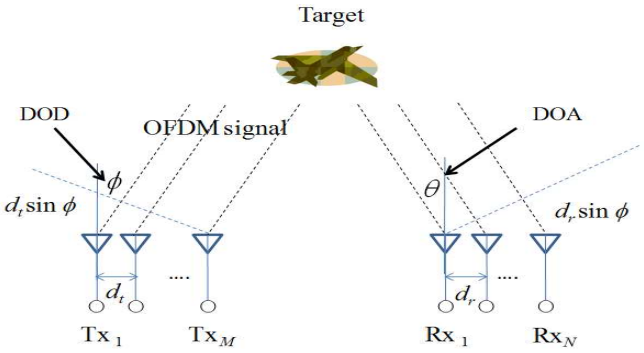

Fig. 1 MIMO radar concept

The proposed scheme adopted an approach in [10] where the radar simultaneously transmits *M* sets orthonormal baseband from vector $\mathbf{S} = [\mathbf{S}_1, \mathbf{S}_2, \ldots, \mathbf{S}_M]$. The resulting baseband signal matrix is expressed by

$$\mathbf{B}(t) = \frac{1}{\sqrt{H}} \sum_{h=0}^{H-1} \mathbf{S} \exp(\, j2\pi f_h t) \tag{1}$$

where f_h is the frequency of the h^{th} sub-carrier. The baseband signal was then converted into the time-domain through inverse Fourier transform, and cyclic prefix is added to each of the OFDM symbols. The addition of the cyclic prefix is known to guarantee the orthogonality of each sub-carrier, which is required by the MIMO radar system [10]. In our scheme, each OFDM symbol is treated as one snapshot of the probing signal, hence the total number of snapshot depends on the number OFDM symbol transmitted. Fig. 2 depicts the OFDM waveform emitted from the *m*th transmitting antenna.

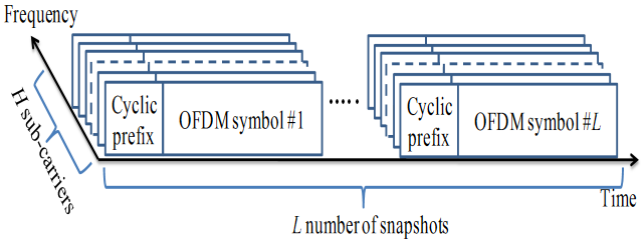

Fig. 2 Composition of the proposed OFDM probing signal emitted from the *m*th transmitting antenna

The spectra of the transmitting baseband matrix is then given by

$$\mathbf{C}(f) = \int_0^T \mathbf{B}(t) \exp(-j2\pi f t)\, dt \tag{2}$$

The spectra of the received signal is expressed by

$$\mathbf{Y}(f) = [\mathbf{a}_t(f,\phi) \otimes \mathbf{a}_r(f,\theta)]\mathbf{C}(f - f_c)g(f) \tag{3}$$

where f_c is the center frequency, g is the reflection coefficient of the target, a_t and a_r are the transmitting and receiving steering vectors, respectively, and $\otimes$ is the kronecker product operator. Down-converting Y(*f*) to the baseband give

$$\mathbf{Y}(t) = \int_0^T \mathbf{Y}(f + f_c)\exp(j2\pi ft)df + \mathbf{n}(t) \quad (4)$$

where n(t) is the thermal noise. Fourier transform of Y(t) after cyclic prefix removal yields the receive code matrix for each sub-carrier U_h = [$U_{1,1}$, $U_{2,2}$, …, $U_{h,N}$], where N is the number of receiving antennas. Multiplying U_h with S^* yields the channel coefficient for each transmitter and receiver pair, denoted as A_h. The receiving co-variance matrix and its Eigen decomposition is given by

$$\mathbf{R}_h = E[\mathbf{A}_h(t)\cdot\mathbf{A}_h(t)^H] \quad (5)$$

where $E[\cdot]$ is the ensemble average and $[\cdot]^H$ represents the conjugate transpose operation. The co-variance matrix is estimated by an average of L number of snapshots. Singular value decomposition of the covariance matrix gives

$$\mathbf{R}_{xx\_h} = \mathbf{E}^{(h)}\mathbf{V}^{(h)}\mathbf{E}^{(h)H} \quad (6)$$

where $\mathbf{V}^{(h)}$ is a diagonal matrix whose diagonal elements contain the signal and noise eigenvalues for the h^{th} sub-carriers, and $\mathbf{E}^{(h)}$ is the corresponding eigenvectors of the signal and noise components. The MUSIC algorithm principle was applied to estimate the DOD and DOA by formulating the pseudo-spectra at each of the sub-carriers. The DOA and DOD at the h^{th} sub-carriers can be jointly estimated by formulating the MUSIC spectrum at the h^{th} sub-carrier, P_h, using two-way MUSIC given by

$$P_h(\phi,\theta) = \frac{1}{[\mathbf{a}_t(\phi)\otimes\mathbf{a}_r(\theta)]^H\mathbf{e}_N\mathbf{e}_N^H[\mathbf{a}_t(\phi)\otimes\mathbf{a}_r(\theta)]} \quad (7)$$

where $\mathbf{e}_N$ contains the eigenvectors of $\mathbf{R}_h$ that are orthogonal to the steering vectors $\mathbf{a}_t$ and $\mathbf{a}_r$. The DOD and DOA are determined by the largest peak in the MUSIC spectrum.

Finally, the wideband DOD and DOA is decided by taking majority decision among estimates at all H sub-carriers. As mentioned in the previous section, we adopted a non-parametric method which utilizes histograms [7] which were formulated from the data array of all the H estimates, which are denoted as 'angle histograms' in the rest of the paper. The angle histogram can be viewed as a function of angle i from -90˚ to 90˚ at intervals of, for example, 0.5˚.

The normalized number of occurrence of the peak angle is then given by

$$\hat{r}^{(i)} = \frac{1}{z}p^{(i)} \quad (8)$$

where $p^{(i)}$ is the number of occurrences of the angle i, and z is the normalized coefficient given by

$$z = \arg\max\ \hat{r}^{(i)} \quad (9)$$

The majority decision is obtained by searching the peak of the histogram, which corresponds to the most occurred angle from the estimation. The above-mentioned steps summarize the base algorithm to estimate wideband DOD and DOA.

As for the adaptive power allocation scheme, the proposed MIMO radar initially estimates the DOD and DOA within the first scan (*e.g.* L = 100 snapshots), followed by a feedback loop to the transmitter. During the initial scan, the system simultaneously constructs a database of singular values against the sub-carrier index, obtained from singular value decomposition (refer Equation (6)) of the receiving co-variance matrix at each respective sub-carrier. The magnitude of the singular values was normalized to the largest singular value among the sub-carriers, and the system then selects 'usable' sub-carriers based on a specific threshold. 'Non-usable' sub-carriers (ones bearing low value of singular values) will be omitted in the next scan by bearing zero-weights when allocating sub-carriers at the transmitter. The total transmitting power is then distributed among the selected sub-carriers to maximize the spectral efficiency. Fig. 3 illustrates the block diagram of the proposed scheme.

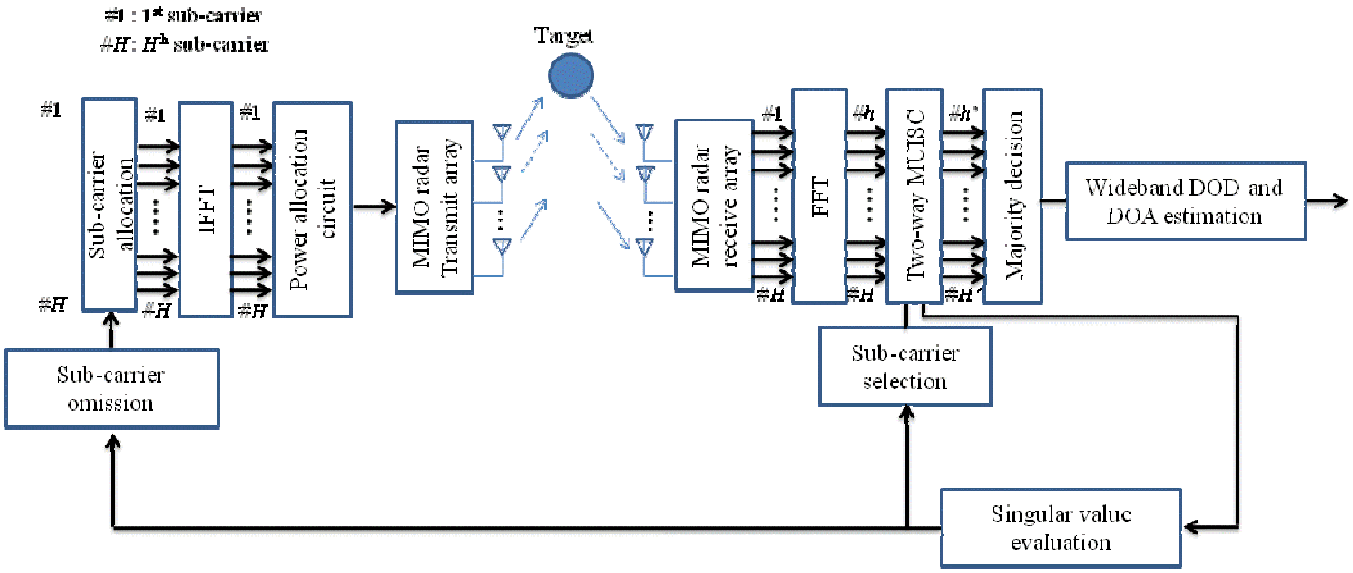

Fig. 3 Block diagram of the proposed scheme

III. Results and Discussion

This section presents the results of numerical simulations, followed by experimental results. Simulations were conducted using commercial signal processing tool MATLAB. The numerical simulations analyse the system performance based on utilization of OFDM waveform 128 number of sub-carriers for the sake of demonstration. The following experimental measurement will show the results when using 128 and 256 sub-carriers, in order to show performance improvement obtained from utilization of a larger number of sub-carriers.

TABLE I
OFDM Waveform Parameters Used in Numerical Simulations

Parameters	**Description**
Center frequency, f_c	3.5 GHz
Total bandwidth	500 MHz
Modulation	BPSK
Total number of sub-carriers	128
Number of data sub-carriers, H	112
Sub-carrier spacing	3.90625
OFDM symbol duration	256 ns
Cyclic prefix	64 ns

A. Simulated Performance

The validity of the proposed scheme was first verified through a series of numerical simulations. A 4×4 MIMO radar, detecting 1 target located at located at (ϕ, θ) = (-20˚, 15˚) was considered. The MIMO radar transmits an OFDM signal with center frequency f_c = 3.5 GHz and the total bandwidth of 500 MHz, which is divided into 128 sub-carriers in the intervals of 3.90625 MHz. 100 OFDM symbol was transmitted to compute the average co-variance matrix in Equation (5) by 100 snapshots. Major parameters of the OFDM signal used are summarized in Table 1. In order to demonstrate the effectiveness of the proposed scheme in utilizing the large number of sub-carriers for the detection of fluctuating target, the target reflection coefficient g was modelled to follow a certain distribution of RCS fluctuations along the frequency domain. It was shown in literature that the measured RCS of automobiles follows Weibull distribution [16], and our internal measurements in radio anechoic chamber confirmed similar distribution along the frequency domain. Therefore, we modelled the coefficient g to yield a probability density function given by

$$f(x) = \begin{cases} 1 - \exp^{-(x/a)^b} & x \geq 0 \\ 0 & x < 0 \end{cases} \quad (10)$$

Here, a and b is the scale and shape parameters, respectively. Random variables were generated to fit the Weibull distribution in the UWB frequency range from 3.1 to 10.6 GHz in intervals of 3.90625 MHz. In the simulation, it was assumed that the target RCS slowly fluctuates, and remained constant within the 100 snapshots.

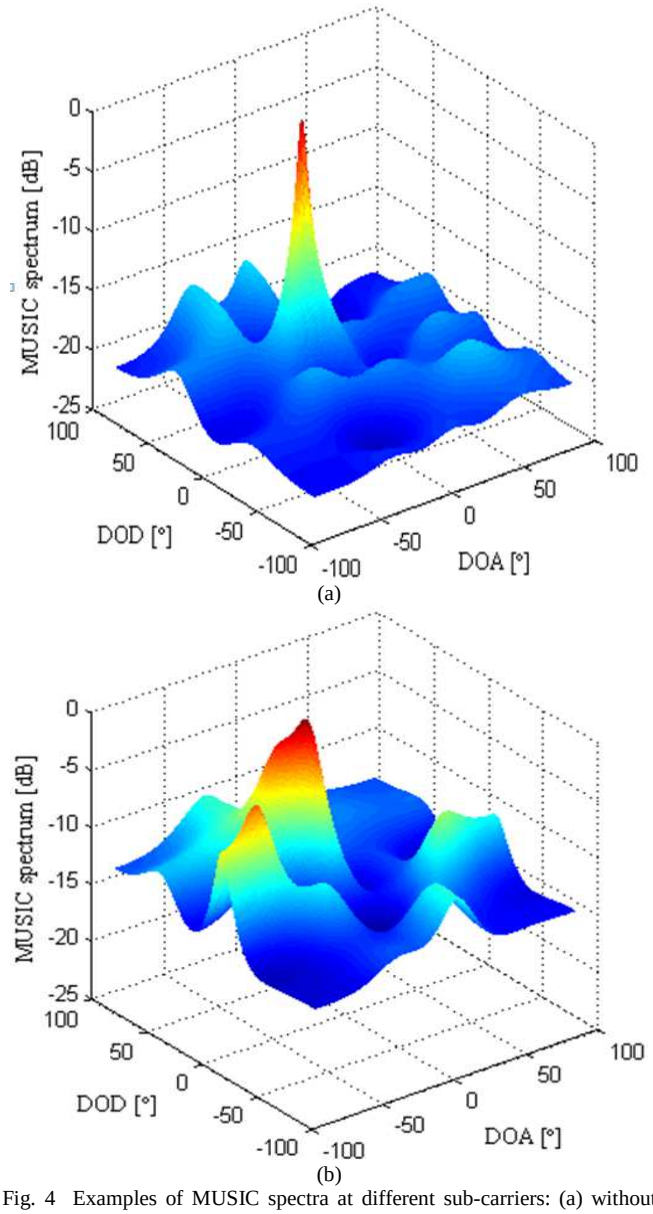

Fig. 4 Examples of MUSIC spectra at different sub-carriers: (a) without RCS fluctuation and (b) 15 dB of RCS fluctuation

Fig. 4 depicts examples of MUSIC spectra at different sub-carriers. It can be observed that RCS fluctuations degraded the quality of the resulting spectra, where it is easily noticeable that spectra in Fig. 4 (a) yielded a sharp peak, while the spectra in Fig. 4 (b) marked a broader peak and larger noise floor. This will induce large estimation errors when formulating the DOD and DOA at the particular sub-carrier. The angle histograms formulated from the estimated DODs and DOAs at all sub-carriers is shown in Fig. 5. It shows the resulting angle histograms of the DOD and DOA when using all the sub-carriers of the OFDM signal. We can observe that besides the peak of the estimated signal, there were spurious plots present in the histograms. These spurious plots were produced from inaccurate estimation in several sub-carriers, due to poor SNR brought by severe RCS fluctuations. Furthermore, the peak of the histograms marked the estimated angles with 0.5˚ (ϕ = -19.5˚) and 1˚ (ϕ = 14˚) error from the actual position of the target.

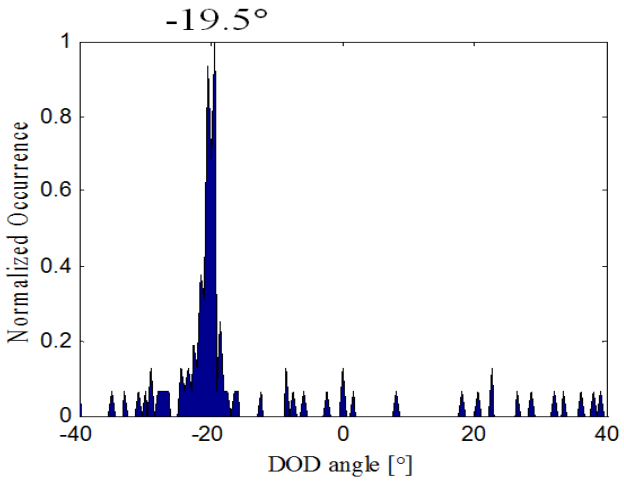

(a)

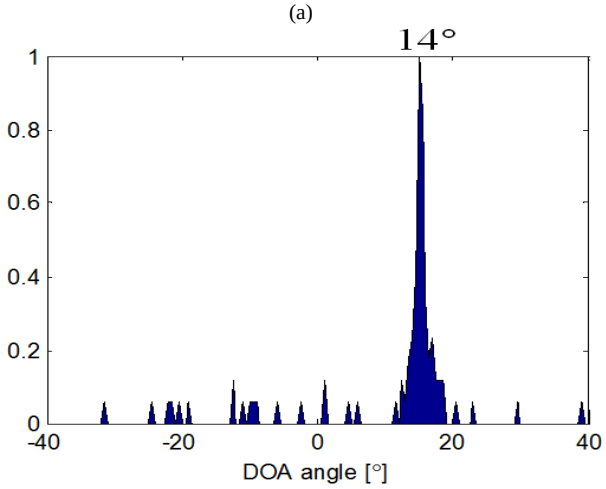

(b)

Fig. 5 Angle histograms simulated using the proposed MIMO OFDM radar without implementation of power allocation scheme (H = 112) : (a) DOD and (b) DOA

The normalized singular values at each sub-carrier are plotted in Fig. 6, where singular values with 1-order smaller values were obtained in several sub-carriers. These sub-carriers can be considered as 'non-usable' sub-carriers, which contributed to the previous spurious and estimation errors. To demonstrate the effectiveness of the proposed adaptive sub-carrier selection method, we selected only the sub-carriers with singular values above the threshold (1.5×10^{-1}) shown in the Fig. 6, where the number of sub-carriers was 70 % of the total. The transmitting signal was modified by inserting zeros in the omitted sub-carriers, and the total signal power was maximized among the selected sub-carriers only. The histograms obtained after implementing the power allocation scheme was plotted in Fig. 7. It was observed in the figure that the estimations after implementing the power allocation scheme yielded better performance against fluctuating targets, compared to without its implementation.

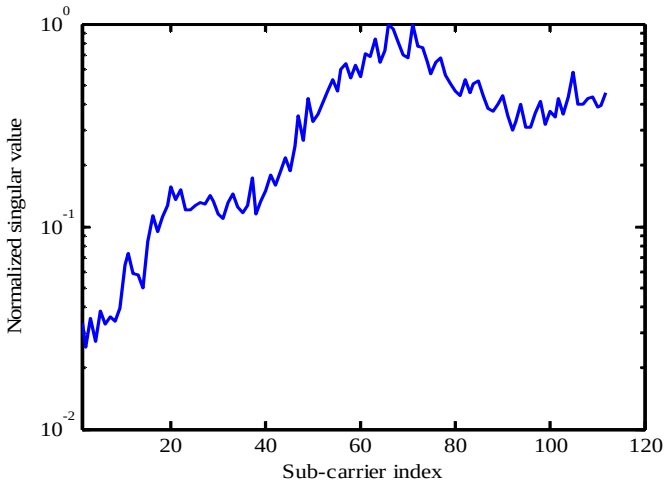

Fig. 6 Normalized singular values at each sub-carrier of the MIMO OFDM radar waveform

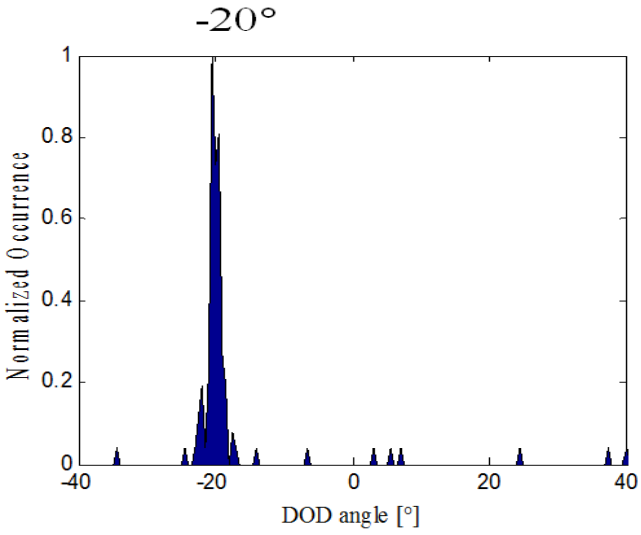

(a)

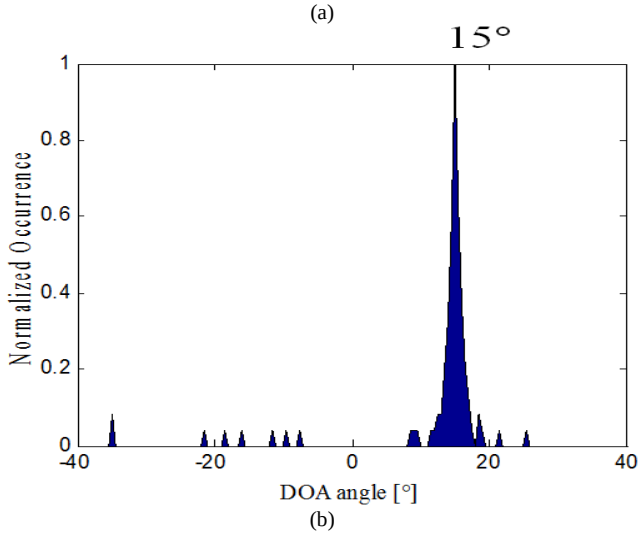

(b)

Fig. 7 Simulated angle histograms after implementation of adaptive power allocation (H = 78): (a) DOD and (b) DOA

B. Experimental Results

An experimental setup as shown in Fig. 8 was developed to validate the proposed algorithm through experimental evaluation in a radio anechoic chamber. Fig. 9 depicts the measurement scenario. The transmitting system was constructed using a combination of an arbitrary waveform

generator (AWG) and quadrature modulators. The baseband OFDM signal was generated using MATLAB, and output through I and Q channels of the AWG with a sampling speed of 2.5 Gs/s. The signals were oversampled 5 times to reduce aliasing and jitter's effects. The signals were then combined and up converted using the quadrature modulator to the center frequency of 3.5 GHz. Wideband horn antennas with an average gain of 12.5 dBi were used as both transmitting and receiving antennas. To construct the MIMO antenna array at both transmitting and receiver sides, electro-mechanical scanners were used to move the horn antennas to pre-determined locations, which corresponds to 4×4 MIMO configuration with spacings of half wavelength. A complex target fabricated using polystyrene and aluminium foil was used to model a fluctuating RCS response against frequency. Fig. 10 shows the frequency response obtained when illuminating the target using the experimental setup. The target was positioned at at (ϕ, θ) = (-15˚, -15˚). The OFDM signal adopted similar parameters used in the previous simulations. The measured spectrum of an OFDM signal impinging the receiver is shown in Fig. 11 (a). We could observe from the figure that the average SNR of the system is approximately 15 dB.

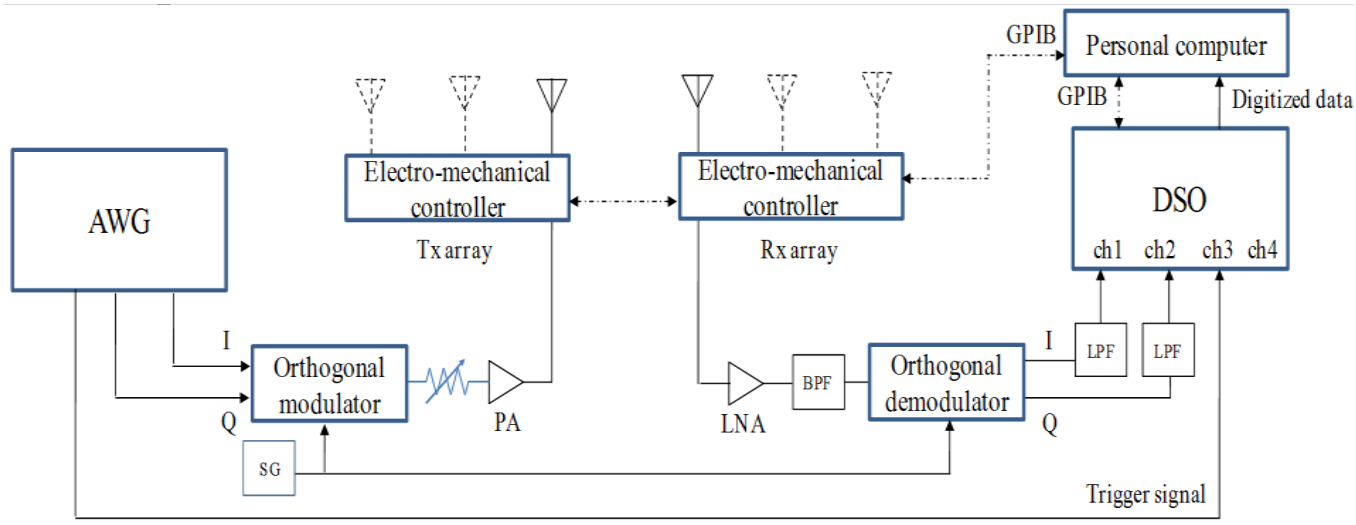

Fig. 8 Experimental setup

Fig. 9 Measurement scenario in a radio anechoic chamber performance against fluctuating targets, compared to without its implementation

The receiving system consists of quadrature demodulators and a digital sampling oscilloscope (DSO). All the received signals captured by the DSO were jointly processed through offline processing routine implemented in MATLAB. Prior to the signal processing routine, the received signal is cross-correlated with the reference signal to detect the start and the end bit. The received signal is then cropped to contain 100 OFDM symbols which equal to 100 snapshots. Fig. 11 (b) shows an example of the captured I and Q channels of the baseband OFDM signal. Subsequently, the signals [19] were down sampled 5 times, and the cyclic prefix is removed before the data can be processed using the proposed scheme [17].

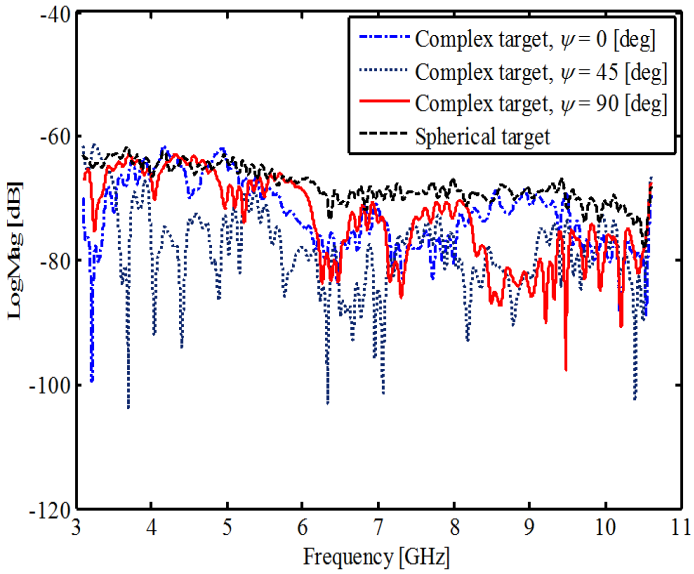

Fig. 10 Frequency response of the fabricated complex target [13]

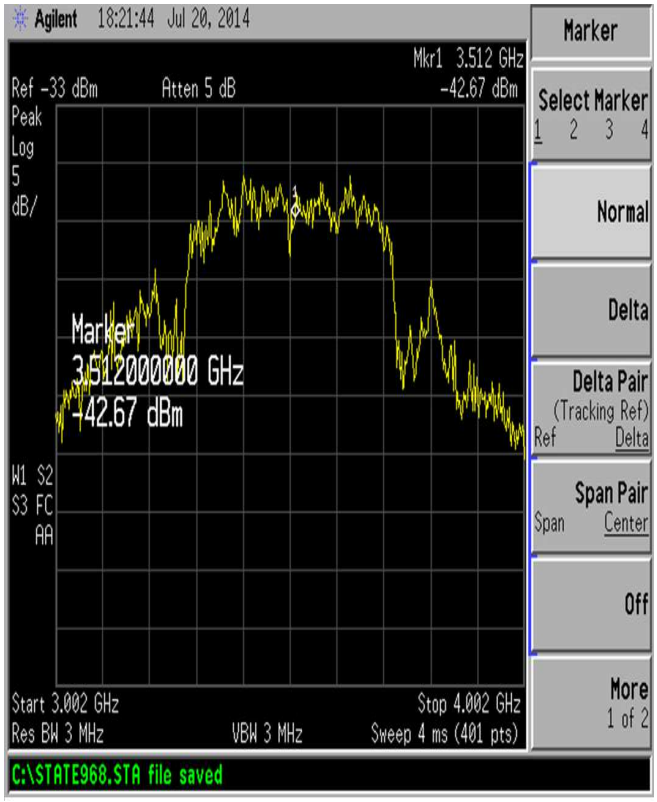

(a)

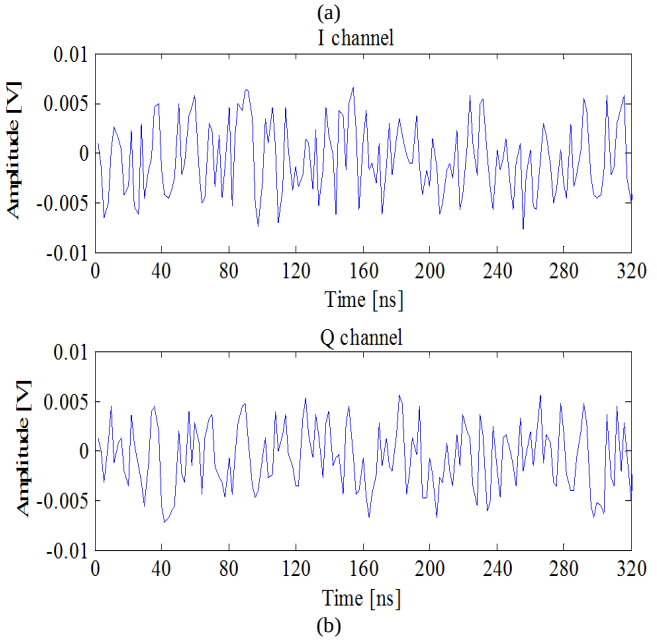

(b)

Fig. 11 Examples of radar signal obtained from the experiment in anechoic chamber: (a) Frequency spectrum of OFDM signal received at the n^{th} receiver (H = 112) and (b) the received baseband signal in the time domain

First, measurement results when using OFDM signal transmitting 128 number of sub-carrier will be analysed. Among the transmitted sub-carriers, a total number of H = 112 number of data sub-carriers were used for angle estimation. The measurement results are shown in Figs. 10 to 12. Fig. 10 shows the angle histograms obtained from the measurement when using all the sub-carriers of the OFDM signal. It can be observed from the peaks of the histograms of the DOD and DOA were -16.5˚ and -17˚ respectively, which corresponded to estimation errors of 1.5˚ and 2˚.

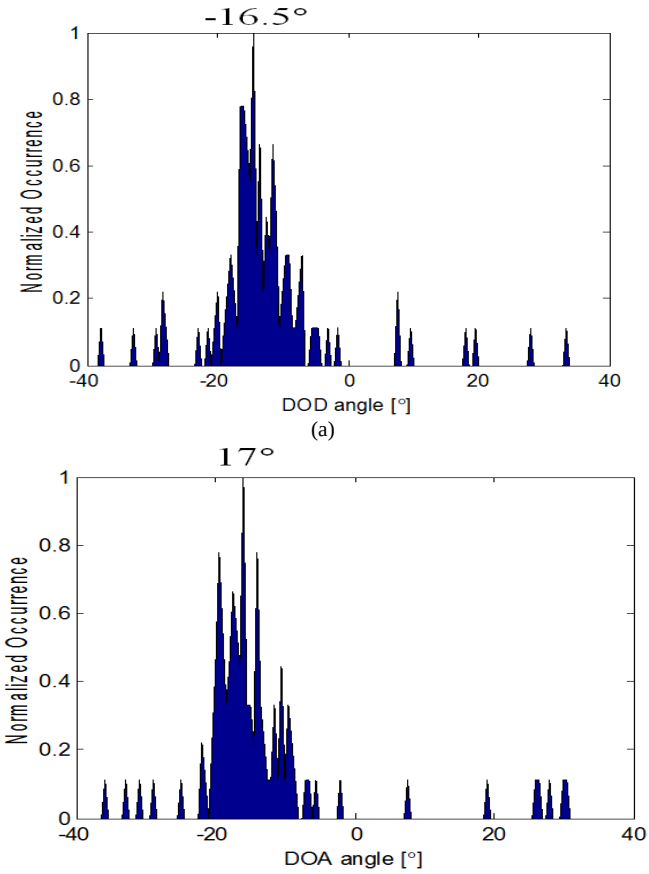

Fig. 12 Angle histograms without power allocation scheme (H = 112): (a) DOD and (b) DOA

The results after implementation of the power allocation scheme are shown in Fig. 13. The sub-carrier selection was implemented based on 70% number of sub-carriers, similarly with the previous simulation. The estimated DOD and DOA with the power allocation scheme were -16˚ and -15˚. The estimation error was reduced to 1˚, and the DOA was estimated with no error. The respective angle histograms were also found to contain a reduced number of spurious. These results verified the performance improvement obtained by the power allocation scheme, as shown in the previous simulations.

Experiments were also conducted by using a larger number of total sub-carriers, and varying threshold values to select the 'usable' sub-carriers. Fig. 13 showed an example of angle histogram, obtained by using 70 % of sub-carriers selected from a total of 256 sub-carriers. It was evident that the angle histograms and estimation accuracy were improved. Several experiments with the plots of the estimation errors versus the number of sub-carriers were shown. The estimation errors were calculated by taking the absolute errors in degree between the actual and estimated angles. The figure indicated an improvement of estimation accuracy with increasing number of sub-carrier used. In summary, both simulations and experimental results showed that the adaptive power allocation scheme produced angle estimation improvements when the radar system was dealing with targets with fluctuating radar cross sections.

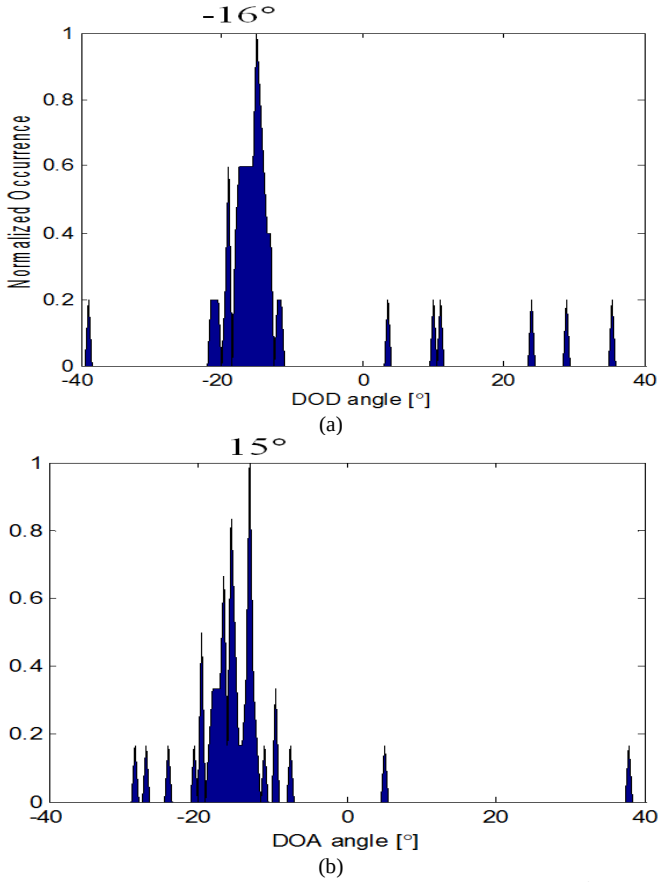

Fig. 13 Angle histograms obtained with implementation of power allocation scheme (H = 78): (a) DOD, and (b) DOA

IV. Conclusion

This paper proposed a target localization scheme in MIMO OFDM radars employing an adaptive power allocation scheme among the sub-carriers. The sub-carrier selection [18] was made by evaluating the singular values (obtained from singular value decomposition) at each of the sub-carrier based on thresholding technique, and the result is fed to the MIMO radar transmitting side. The radar will allocate the transmitting power among the selected sub-carriers from the next scan and onwards. It was shown by numerical simulations and experimental measurements that the proposed scheme was effective in estimating the angles of a target with fluctuating RCS against frequency, ascribed to the utilization frequency diversity obtain from selected sub-carriers of the OFDM signal. Experimental evaluation in a radio anechoic chamber was also done to validate the proposed scheme. The result in this paper was presented in the case of one target, but in principle, it can be applied to multi-targets as well due to the capability of the MUSIC algorithm. The proposed algorithm was considered to be a good candidate to be applied in future MIMO radar systems designed to detect targets with fluctuating radar cross sections.

Acknowledgment

The authors would like to acknowledge Universiti Teknologi MARA for providing the funds to conduct studies related to the work presented in this paper, through Prototype Research Grant Scheme (PRGS), Grant number 600-IRMI/PRGS 5/3 (0005/2016).

References

[1] I. Bekkerman and J. Tabrikian, "Target detection and localization using MIMO radars and sonars," *IEEE Transactions on Signal Processing*, vol. 54, pp. 3873-3883, Oct. 2006.

[2] L. Jian and P. Stoica, "MIMO radar with colocated antennas," *IEEE Signal Processing Magazine*, vol. 24, pp. 106-114, Sep. 2007.

[3] M. A. Hadi, S. Alshebeili, F. E. Abd El-Samie, and K. Jamil, "Compressive sensing for improved MIMO radar performance-A review," in *Proc. ICTRC'15*, 2015, p. 270.

[4] H. Zang, S. Zhou, X. Lv, Y. Cao, L. Xu, and H. Liu, "Joint optimization of waveforms and transmit array for colocated MIMO radar," in *Proc. IEEE RC'15*, 2015, p. 374.

[5] W. Q. Wang, "Virtual antenna array analysis for MIMO synthetic aperture radars," *International Journal of Antennas and Propagation*, vol. 2012, pp. 1-10, Jan. 2012.

[6] F. K. W. Chan, H. C. So, L. Huang, and L. T. Huang, "Parameter estimation and identifiability in bistatic multiple-input multiple-output radar," *IEEE Transactions on Aerospace and Electronic Systems*, vol. 51, pp. 2047-2056, Jul. 2015.

[7] Z. Xiaofei, X. Lingyun, X. Lei, and X. Dazhuan, "Direction of Departure (DOD) and Direction of Arrival (DOA) estimation in MIMO radar with reduced-dimension MUSIC," *IEEE Communications Letters*, vol. 14, pp. 1161-1163, Dec. 2010.

[8] Y. Bobin, W. Wenjie, and Y. Qinye, "DOD and DOA estimation in bistatic non-uniform multiple-input multiple-output radar systems," *IEEE Communications Letters*, vol. 16, pp. 1796-1799, Nov. 2012.

[9] L. Fulai and W. Jinkuan, "AD-MUSIC for jointly DOA and DOD estimation in bistatic MIMO radar system," in *Proc. ICCDA'10*, 2010, p. 455.

[10] X. H. Wu, A. A. Kishk, and A. W. Glisson, "MIMO-OFDM radar for direction estimation," *IET Radar, Sonar and Navigation*, vol. 4, pp. 28-36, Feb. 2010.

[11] K. C. Wee, L. Bin, L. Y. Chang, and M. Y. W. Chia, "MIMO-OFDM radar array configuration for resolving DOA ambiguity," in *Proc. IEEE ICCS'12*, 2012, p. 85.

[12] S. Bin, W. Xuezhi, B. Moran, and L. Xiang, "Target tracking using range and RCS measurements in a MIMO radar network," in *Proc. IET IRC'13*, 2013, p. 1.

[13] I. Pasya, N. Iwakiri, and T. Kobayashi, "Joint direction-of-departure and direction-of-arrival estimation in a UWB MIMO radar detecting targets with fluctuating radar cross sections," *International Journal of Antennas and Propagation*, vol. 2014, pp. 1-15, Jul. 2014.

[14] P. D. Silva and C. K. Seow, "Performance of MIMO radar using two-way MUSIC," in *Proc. PIERS'13*, 2013, p. 84.

[15] M. Fujimoto, S. Ohaka, and T. Hori, "DOA estimation without antenna characteristics calibration for UWB signal by using sub-band processing," in *Proc. IEEE ICWITS'10*, 2010, p. 1.

[16] W. Buller, B. Wilson, L. van Nieuwstadt, and J. Ebling, "Statistical modelling of measured automotive radar reflections," in *Proc. IEEE IIMTC'13*, 2013, p. 349.

[17] X. G. Xia, T. Zhang, and L. Kong, "MIMO OFDM radar IRCI free range reconstruction with sufficient cyclic prefix," *IEEE Transactions on Aerospace and Electronic Systems*, vol. 51, pp. 2276-2293, Jul. 2015.

[18] I. M. Yassin, A. Zabidi, M. S. A. M. Ali, N. M. Tahir, H. A. Hassan, H. Z. Abidin, and Z. I. Rizman, "Binary particle swarm optimization structure selection of nonlinear autoregressive moving average with exogenous inputs (NARMAX) model of a flexible robot arm," *International Journal on Advanced Science, Engineering and Information Technology*, vol. 6, pp. 630-637, Oct. 2016.

[19] M. N. M. Nor, R. Jailani, N. M. Tahir, I. M. Yassin, Z. I. Rizman, and R. Hidayat, "EMG signals analysis of BF and RF muscles in autism spectrum disorder (ASD) during walking," *International Journal on Advanced Science, Engineering and Information Technology*, vol. 6, pp. 793-798, Oct. 2016.